Supporting Information

Interfacial modulation of Ru catalysts by B, N co-doped porous carbon-confined MoC quantum dots for enhanced hydrogen evolution reaction performance

Shumin Xie[a,1], Mang Niu[a,1], Xingyun Li[a, *], Yang Lei[b], Huanfang Zhang[a], Shuai Xu[a], Deyu Wang[c], Sameh M. Osman[d], Zhi Peng[a], and Yusuke Yamauchi[e,f,g *]

[a]Institute of Materials for Energy and Environment, College of Materials Science and Engineering, Qingdao University, Qingdao 266071, China

[b]School of Chemistry and Chemical Engineering, Hubei Key Laboratory of Coal Conversion and New Carbon Materials, Wuhan University of Science and Technology, Wuhan 430081, China

[c]Key Laboratory of Optoelectronic Chemical Materials and Devices of Ministry of Education, Jianghan University, Wuhan 430056, China

[d]Chemistry Department, College of Science, King Saud University, P. O. Box 2455, Riyadh 11451, Saudi Arabia

[e]Department of Materials Process Engineering, Graduate School of Engineering, Nagoya University, Nagoya 464-8603, Japan

[f]Australian Institute for Bioengineering and Nanotechnology (AIBN), The University of Queensland, Brisbane, Queensland 4072, Australia

[g]Department of Plant & Environmental New Resources, College of Life Sciences, Kyung Hee University, 1732 Deogyeong-daero, Giheung-gu, Yongin-si, Gyeonggi-do 17104, South Korea

Calculation method

The DFT calculations were carried out using the Vienna Ab-initio Simulation Package (VASP)[1, 2] with the frozen-core all-electron projector-augment-wave (PAW)[3, 4] method. The Perdew-Burke-Ernzerhof (PBE)[5] of generalized gradient approximation (GGA) was adopted to describe the exchange and correlation potential. The cutoff energy for the plane-wave basis set was set to 450 eV. A mono-layer 8×8 graphene was used, and a vacuum region of 20 Å above it was used to ensure the decoupling between neighboring systems. N-doped graphene (NC) was simulated by inducing 2-pyrrolic N, 3-pyridinic N, and 3-graphitic N in the graphene. The Ru_{13} and 2-layer 3×3 MoC (111) clusters were placed on the NC to built Ru/NC and MoC/NC composites, respectively. Both of Ru_{13} and MoC cluster was placed on the NC to built Ru/MoC@NC composite, and 2-C atoms of NC were replaced by 2-B atoms was used to simulate the models of B-N-co-doped graphene (BNC). The geometry optimizations were performed until the forces on each ion was reduced below 0.01 eV/Å, and a 1×1×1 Monkhorst-Pack k-point[6] sampling of the Brillouin zone was used. The DFT-D3 method were used to describe the van der Waals interaction[7].

The Gibbs free-energy (ΔG) is calculated as

$$\Delta G = E_{DFT} + \Delta E_{ZPE} - T\Delta S$$

ΔE_{ZPE} is the difference corresponding to the zero point energy between the adsorbed molecule and molecule in the gas phase and ΔS is one molecule entropy between absorbed state and gas phase. E_{DFT} is the total energy of DFT calculated system.

The formation energy (E_f) of Ru_{13} cluster on MoC@BNC substrate was calculated by the following equation:

$E_f = E_{Ru/MoC@/BNC} - E_{MoC@BNC} - E_{Ru}$

where $E_{Ru/MoC@BNC}$ is the total energy of Ru/MoC@/BNC, $E_{MoC@BNC}$ is the total energy of MoC@BNC substrate, and E_{Ru} is the total energy of Ru_{13} cluster.

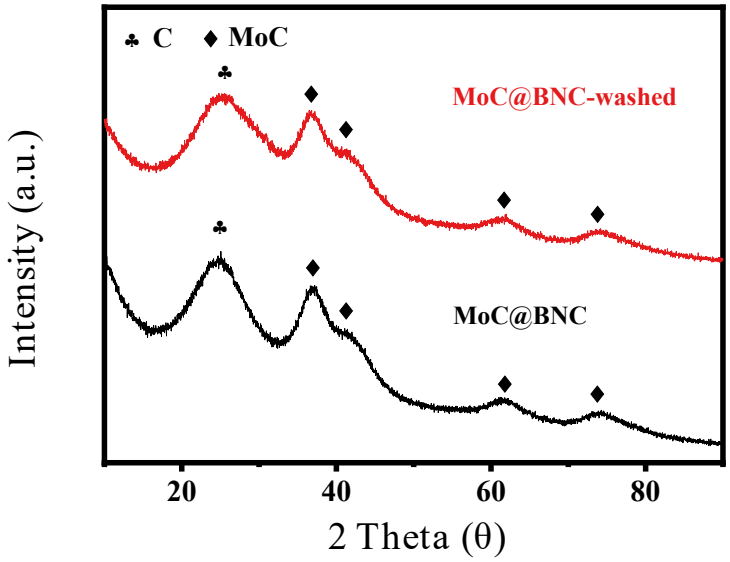

Fig. S1 XRD patterns of MoC@BNC samples before and after methanol washing.

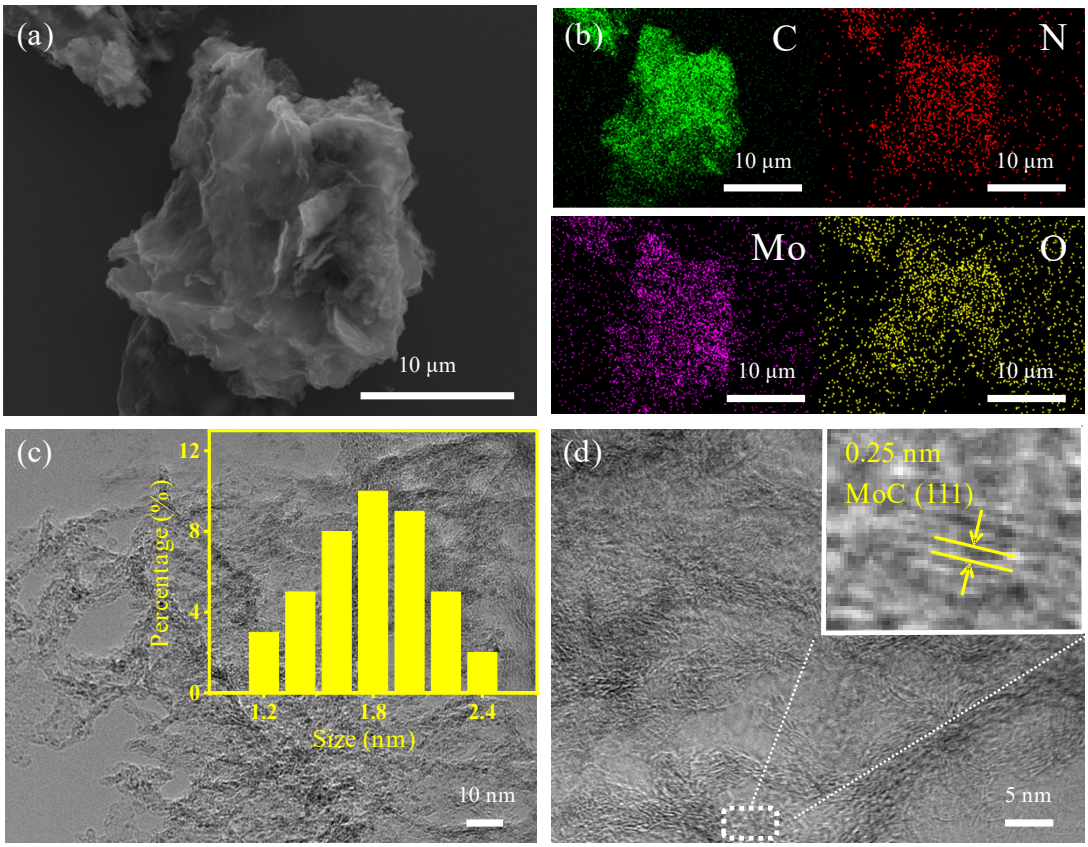

Fig. S2 (a) SEM image, (b) EDS elemental mapping of C, N, Mo, and O, (c) TEM image (inset is the particle size distribution of MoC), and (d) HR-TEM image of MoC@NC.

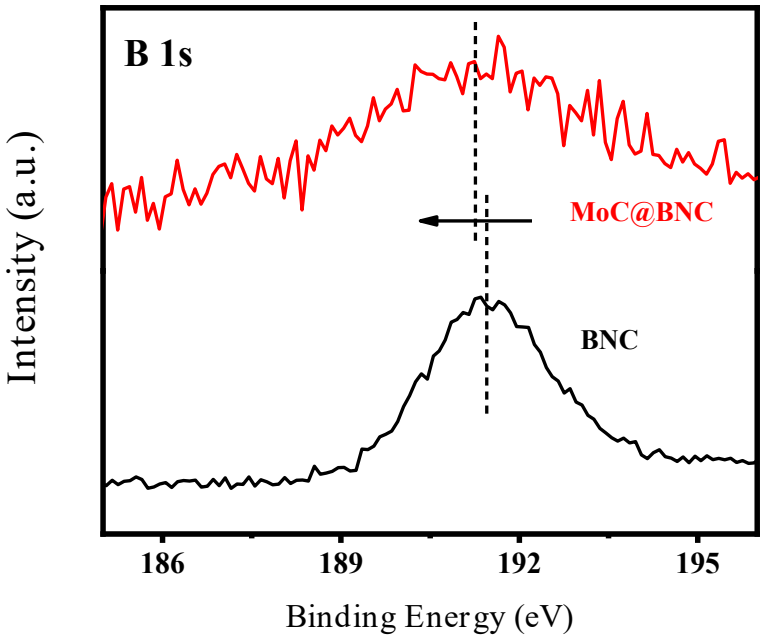

Fig. S3 B 1*s* XPS spectra of MoC@BNC and BNC.

Table S1 The loadings of Ru and Mo on various samples analyzed by ICP-OES.

Material	Ru *(wt.%)*	Mo *(wt.%)*
Ru/MoC@BNC	4.0	17.0

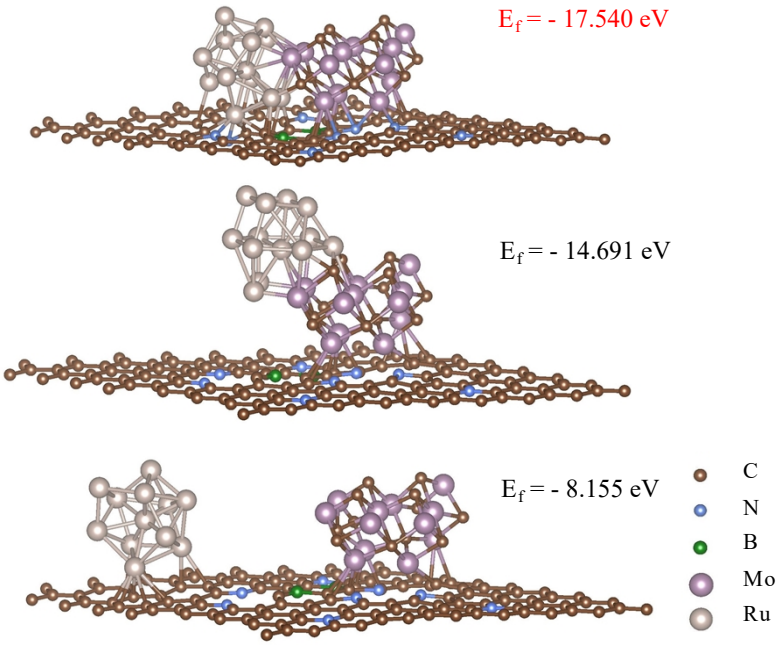

Fig. S4 The optimized structures of Ru_{13} cluster on the surface of MoC@BNC substrate and the corresponding formation energy (E_f).

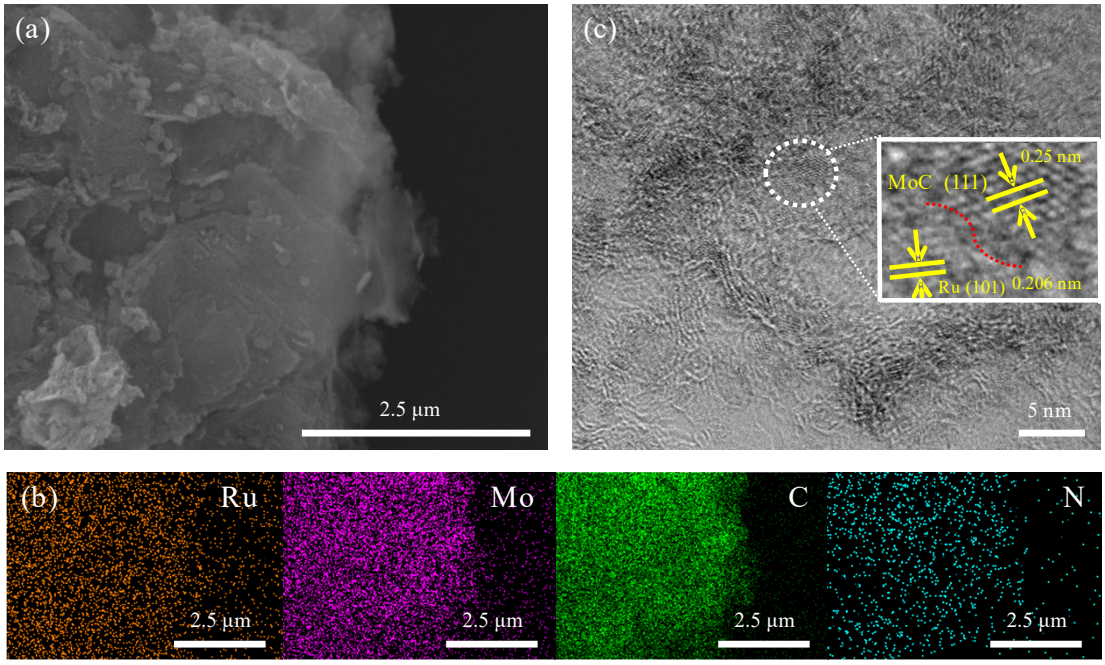

Fig. S5 (a) SEM image, (b) EDS elemental mapping of Ru, Mo, C, and N, and (c) TEM image of Ru/MoC@NC.

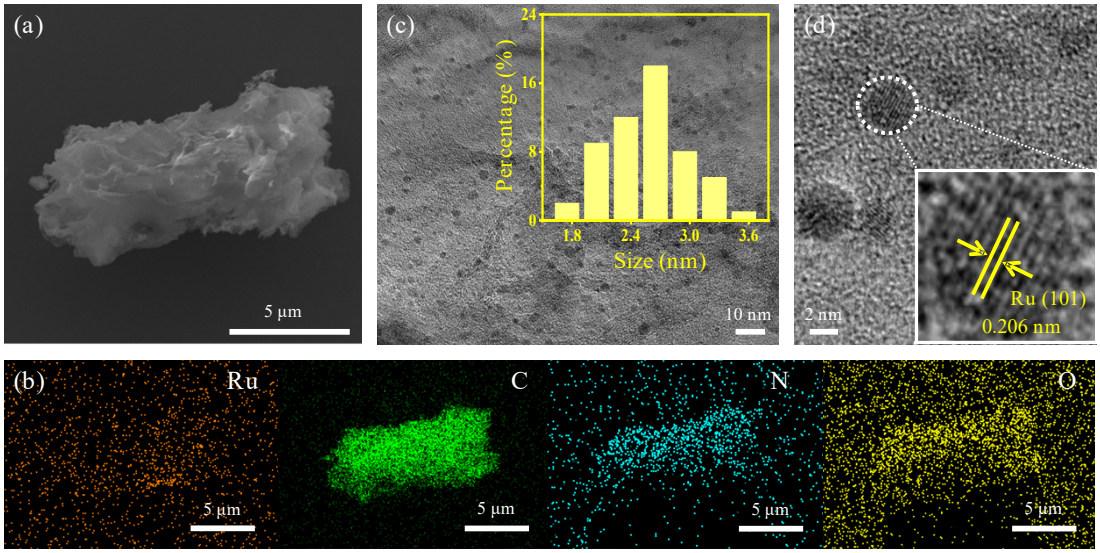

Fig. S6 (a) SEM image, (b) EDS elemental mapping of Ru, C, N, and O, and (c-d) TEM image of Ru/NC.

Table S2 Porosity parameters of Ru/MoC@BNC, Ru/MoC@NC, and Ru/NC obtained from N_2 adsorption desorption isotherms.

Materials	S_{BET} (m^2/g)	V^a_{total} (cc/g)
Ru/MoC@BNC	227.0	1.29
Ru/MoC@NC	218.3	1.20
Ru/NC	250.0	1.11

[a] total pore volume at P/P_0= 0.99.

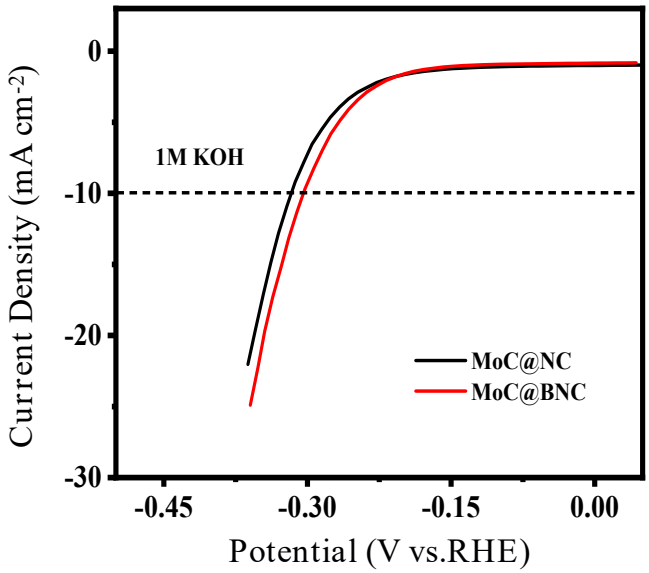

Fig. S7 Polarization curve of MoC@BNC and MoC@NC in 1.0 M KOH electrolyte at 5 mV s^{-1}.

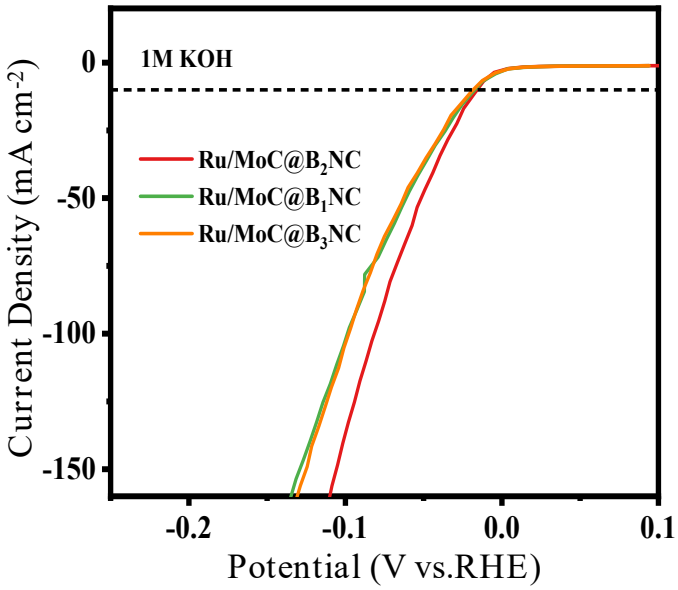

Fig. S8 Polarization curve of Ru/MoC@BNC of different B contents in 1.0 M KOH electrolyte at 5 mV s^{-1}.

Table S3 Comparison of η_{10} and tafel slope of Ru/MoC@BNC with representatively reported HER electrocatalysts.

Catalysts	Overpotential at 10 mA cm^{-2} (mV)	Ref.
Ru/MoC@BNC	14	This work
Ru NCs/NC	14	8
Mo-Ru NSAs	16	9
TNCR-600	17	10
B-Ru@CNT	17	11
Mo_2C-Ru@CNBs	18	12
P, Mo-Ru@PC	21	13
RuNi/MoC@NC	21	14
Ru@WNO-C	24	15
Ru/α-MoC	25	16
Ru/NBC	30	17
Ru/BN@C	32	18
Ru-Mo_2C/CN	34	19
Mo-Ru/CNTs	35	20
Ru/TiN-300	38	21
Mo-RuCoOx	41	22
Ru SAs/N-Mo_2C NSs	43	23

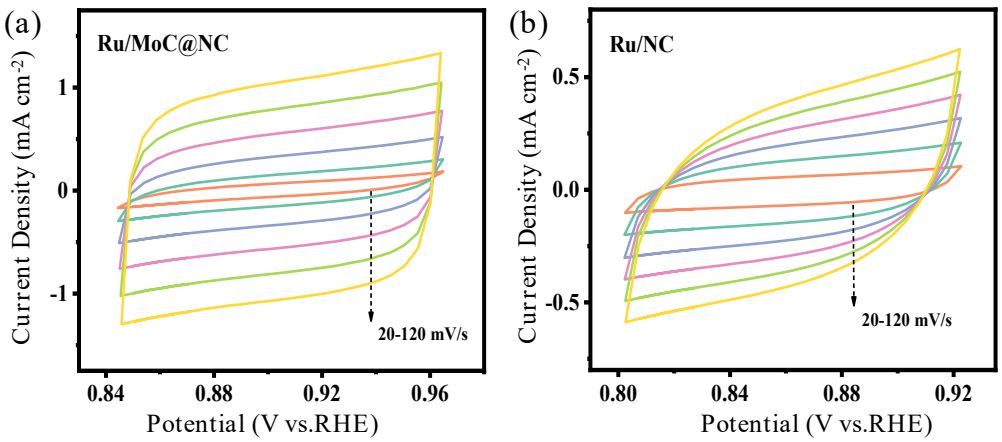

Fig. S9 Cyclic voltammogram of Ru-based catalysts with different rates from 20 to 120 mV s^{-1}.

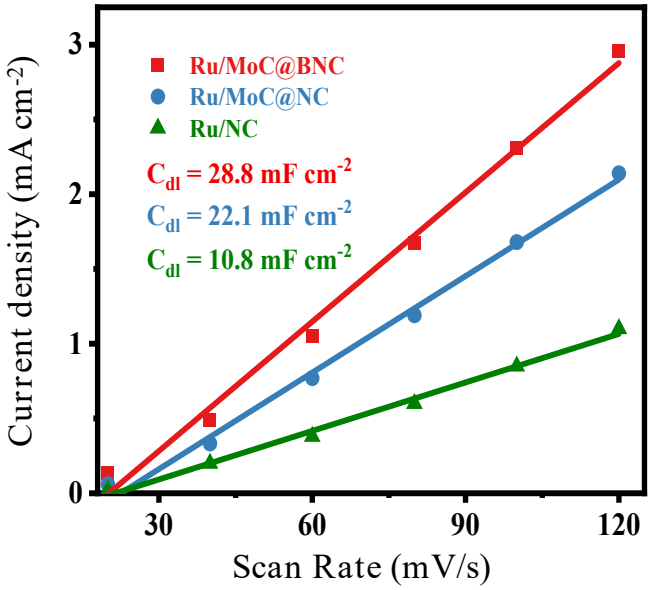

Fig. S10 The capacitive current at 0.1 V as a function of scan rate for Ru/MoC@BNC, Ru/MoC@NC, and Ru/NC.

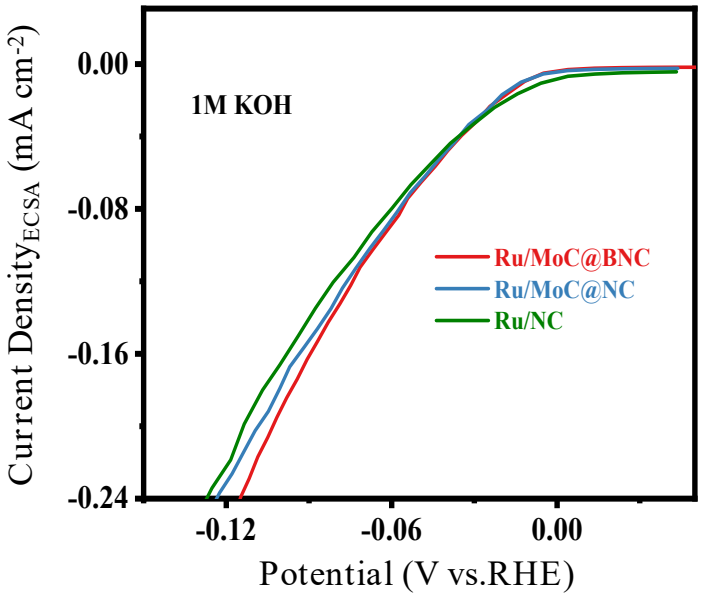

Fig. S11 Polarization curves normalized by ECSA for the Ru/MoC@BNC, Ru/MoC@NC and Ru/ NC.

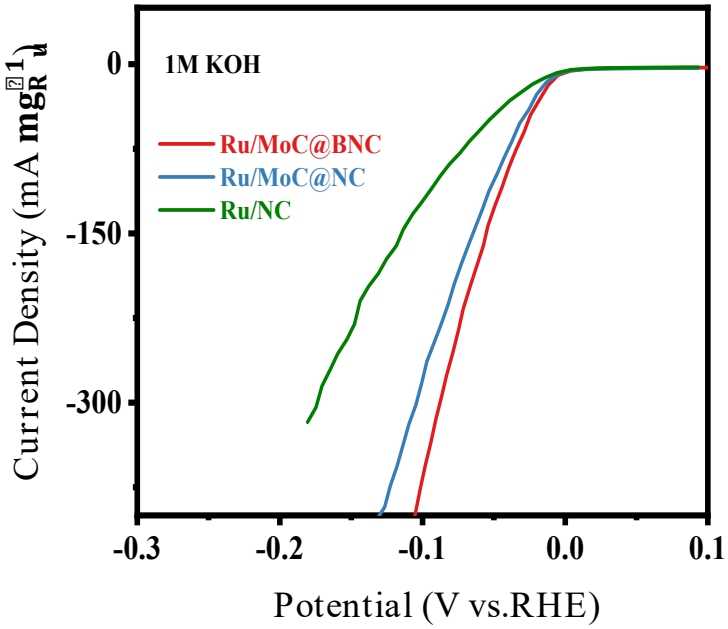

Fig. S12 Polarization curve of Ru/MoC@BNC, Ru/MoC@NC and Ru/NC in 1.0 M KOH electrolyte at 5 mV s^{-1} (the unit of current density is mA mg_{Ru}^{-1}).

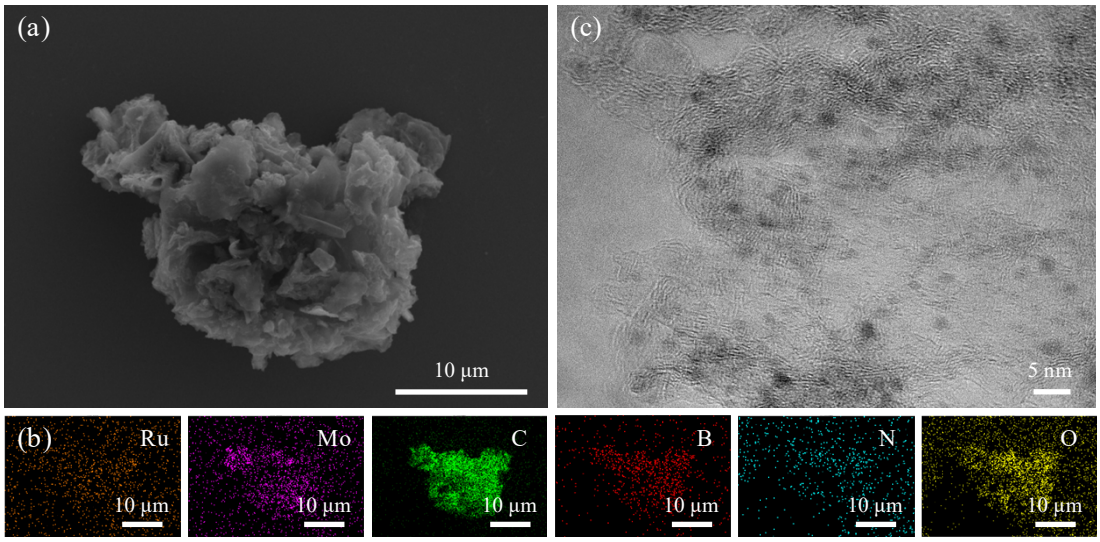

Fig. S13 (a) SEM image, (b) Ru, Mo, C, B, N, and O EDS elemental mapping and (c) TEM image of Ru/MoC@BNC following the durability test.

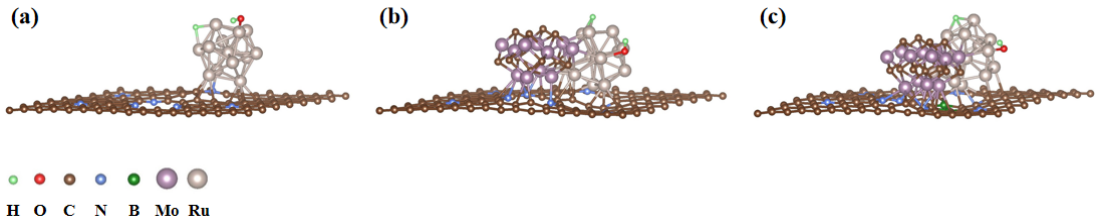

Fig. S14 Optimized adsorption structures of *OH+*H for (a) Ru/NC, (b) Ru/MoC@NC, and (c) Ru/MoC@BNC.

References

1. G. Kresse and J. Hafner, *Phys. Rev. B*, 1994, **49**, 14251-14269.
2. G. Kresse and J. Furthmu¨ller, *Phys. Rev. B*, 1996, **54**, 11169-11186.
3. P. E. Blöchl, *Phys. Rev. B*, 1994, **50**, 17953-17979.
4. G. Kresse and D. Joubert, *Phys. Rev. B*, 1999, **59**, 1758-1775.
5. B. Hammer, L. B. Hansen and J. K. Norskov, *Phys. Rev. B*, 1999, **59**, 7413-7421.
6. H. J. Monkhorst and J. D. Pack, *Phys. Rev. B*, 1976, **13**, 5188-5192.
7. S. Grimme, J. Antony, S. Ehrlich and H. Krieg, *J. Chem. Phys.*, 2010, **132**, 154104.
8. X. Huang, R. Lu, Y. Cen, D. Wang, S. Jin, W. Chen, I. Geoffrey, N. Waterhouse, Z. Wang, S. Tian and X. Sun, *Nano Res.*, 2023, **16**, 9073-9080.
9. L. Li, S. Liu, C. Zhan, Y. Wen, Z. Sun, J. Han, T.-S. Chan, Q. Zhang, Z. Hu and X. Huang, *Energy Environ. Sci.*, 2023, **16**, 157-166.
10. M. Wu, X. Fan, W. Zhang, B. Chen, T. Ye, Q. Zhang, Y. Fang, Y. Wang and Y. Tang, *Chin. Chem. Lett.*, 2024, **35**, 109258.
11. X. Sun, W. Li, J. Chen, X. Yang, B. Wu, Z. Wang, B. Li and H. Zhang, *J.*

Colloid Interface Sci., 2022, **616**, 338-346.

12. B. Qin, C. He, Y. Wei, L. Ji, T. Wang, Z. Chen and S. Wang, *Electrochim. Acta*, 2023, **444**, 141977.
13. C. Li, H. Jang, S. Liu, M. G. Kim, L. Hou, X. Liu and J. Cho, *Adv. Energy Mater.*, 2022, **12**, 2200029.
14. X. Fan, B. Li, C. Zhu, F. Yan and Y. Chen, *Nanoscale*, 2023, **15**, 16403-16412.
15. G. Meng, H. Tian, L. Peng, Z. Ma, Y. Chen, C. Chen, Z. Chang, X. Cui and J. Shi, *Nano Energy*, 2021, **80**, 105531.
16. X. Fan, C. Liu, M. Wu, B. Gao, L. Zheng, Y. Zhang, H. Zhang, Q. Gao, X. Cao and Y. Tang, *Appl. Catal. B: Environ.*, 2022, **318**, 121867.
17. B. Jiang, Z. Wang, H. Zhao, X. Wang, X. Mao, A. Huang, X. Zhou, K. Yin, K. Sheng and J. Wang, *Nanoscale*, 2023, **15**, 19703-19708.
18. A. Salah, H. D. Ren, N. Al-Ansi, H. Tan, F. Yu, L. Yanchun, B. M. Thamer, A. Al-Salihy, L. Zhao and Y. Li, *J. Colloid Interface Sci.*, 2023, **644**, 378-387.
19. J. Chen, C. Chen, Y. Chen, H. Wang, S. Mao and Y. Wang, *J. Catal.*, 2020, **392**, 313-321.
20. J. Sun, Z. Zhao, Z. Li, Z. Zhang, R. Zhang and X. Meng, *J. Mater. Chem. A*, 2023, **11**, 22430-22440.
21. X. Wang, X. Yang, G. Pei, J. Yang, J. Liu, F. Zhao, F. Jin, W. Jiang, H. Ben and L. Zhang, *Carbon Energy*, 2023, **6**, e391.
22. Y. Zhang, R. Lu, C. Wang, Y. Zhao and L. Qi, *Adv. Funct. Mater.*, 2023, **33**, 2303073.

23. J. Yu, A. Wang, W. Yu, X. Liu, X. Li, H. Liu, Y. Hu, Y. Wu and W. Zhou, *Appl. Catal. B: Environ.*, 2020, **277**, 119236.